3 WAG-3 OU 3-13 RI/BRA AQUIFER MODEL SENSITIVITY TO INTERBED PARAMETERIZATION

Only a limited amount of empirical data is available to confirm the physical properties of the HI interbed as assumed in the OU 3-13 RI/BRA model and there is no data regarding the presence or absence of contaminants in the interbed. Empirical evidence of the HI interbed contamination and permeability is required to verify the model predictions and refine the model parameterization. In the event that observed concentrations exceed the action levels defined in the WAG-3 Record of Decision, an updated numerical model will be used to guide remediation efforts. Sensitivity of the model parameterization was performed to identify key data needs, support field activities to collect empirical data, and help estimate the uncertainty of the RI/BRA model.

3.1 HI Interbed Discretization Sensitivity

The OU 3-13 aquifer model has been rediscretized to determine the RI/BRA model's sensitivity to the simulated aquifer depth and the number of model layers used to represent the HI interbed. The OU 3-13 RI/BRA simulations indicated the HI interbed was primarily responsible for maintaining elevated I-129 concentrations. The RI/BRA model treats the vertical component of the HI interbed as a single numerical grid block of constant (7.6 m) thickness. This one grid block discretization averages concentrations throughout the entire depth of the interbed and does not allow a vertical concentration gradient to exist in the interbed. This effect may allow an artificially large amount of mass to enter the interbed. As a general rule, lithological structures of very different hydrologic properties should be represented by at least 3 model layers.

The OU 3-13 aquifer model also used a uniform 76 m total thickness, which placed the model's bottom surface either above or below the interbed. Placement of the OU 3-13 model's bottom surface above the HI interbed's lowest point presents potential for erroneous low or high velocity areas due to extreme confining conditions, which are the result of the numerical grid. The updated model's bottom surface was created from flowing aquifer thickness estimates provided by Dr. Smith (personal communication, 2000). Dr. Smith used deep well temperature logs to estimate flowing aquifer thickness. The isothermal temperature gradient in the temperature logs suggest cold recharge water is moving fast enough to overcome the geothermal gradient and identify the actively flowing portion of the aquifer. The number of deep wells which fully penetrate the aquifer is limited and a large amount of interpolation was needed to create the model's bottom surface. Figure 3-1 illustrates deep well locations and the flowing aquifer thickness at each well. The updated model's bottom surface is below the HI interbed at all locations within the simulation domain and does not present the possibility of extreme confining conditions. The temperature log from well UGSG-22 indicates the aquifer is not moving at this location and the effective thickness is zero. Figure 3-2 illustrates the simulated aquifer thickness in the updated model. The surface illustrated in Figure 3-2 is one of many possible realizations of the active aquifer depth in the vicinity of the INTEC.

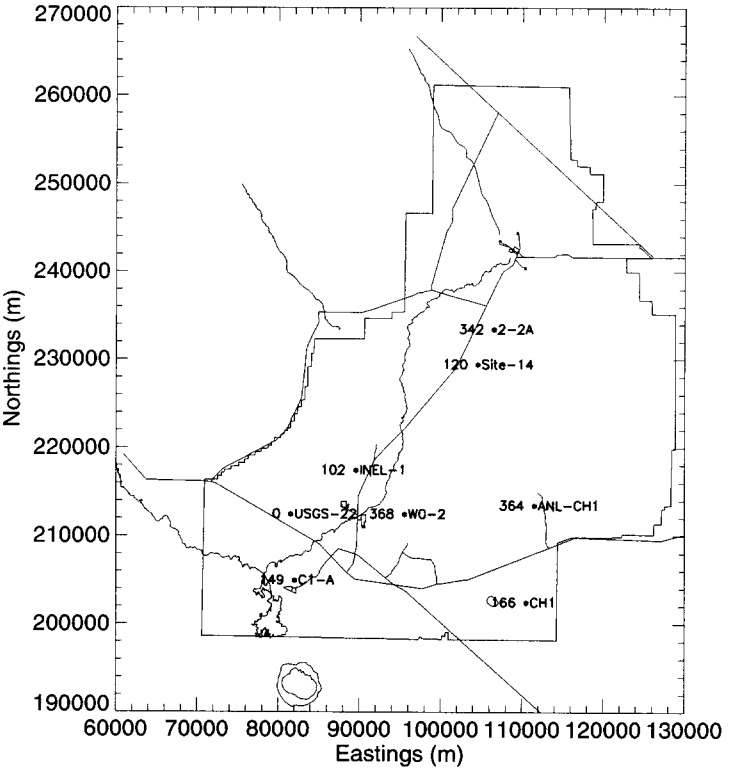

Figure 3-1 INEEL deep wells locations with flowing aquifer depth (m).

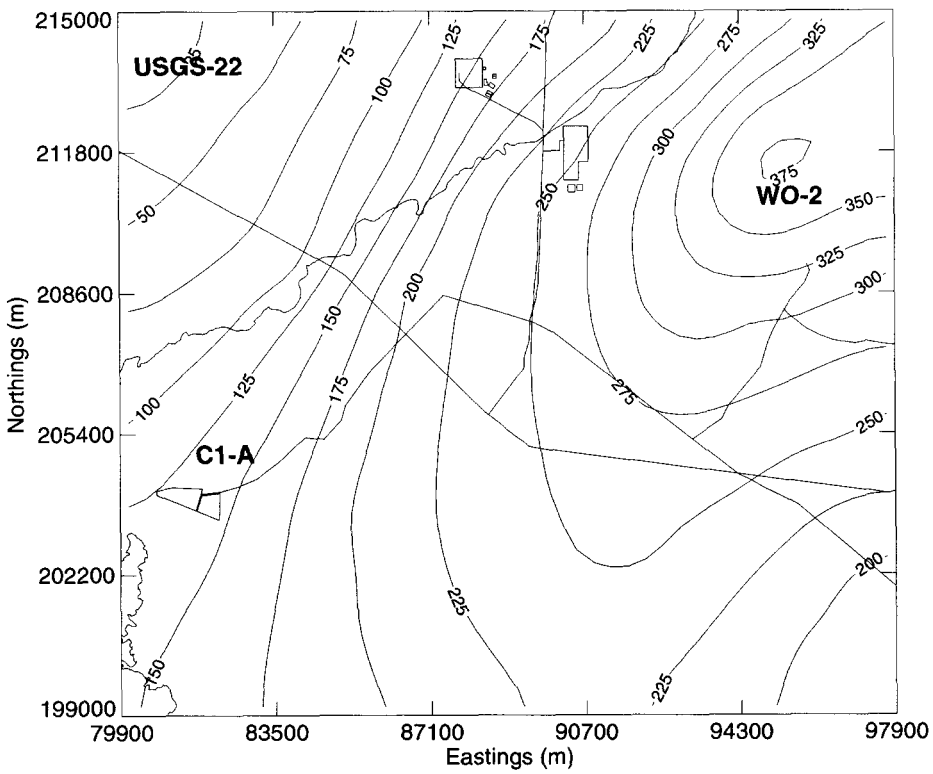

Figure 3-2 Updated aquifer model thickness (m).

3.1.1 HI Interbed Placement

HI interbed elevation and thickness data for placement of the HI interbed were reviewed and incorporated into the updated aquifer model.

3.1.1.1 HI Interbed Depth and Thickness

The HI interbed is a widespread layer of clay and silt overlying basalt flow group I. The interbed tends to dip in the south-east direction when viewed from a large scale (OU 3-13 RI/BRA aquifer model domain) and the interbed tends to become thicker and more continuous in the south-east direction. Well logs from wells SPERT-IV and Site-09 (south-east of INTEC) indicate the interbed can be approximately 27 m thick in some areas.

Data from 51 wells were used to described the HI interbed thickness and surface elevation. Planes were fitted through both surface elevation and thickness data sets. Detrended data sets of the surface and thickness were created by subtracting the fitted planes. Variogram models describing spatial correlation were then fitted to the detrended data and Kriging was used to create the model HI interbed structure. The data used to create the HI interbed is contained in Table 3-1. Figures 3-3 and 3-4 illustrate interbed thickness and Figures 3-5 and 3-6 illustrate interbed elevation surfaces. Figures 3-3 through 3-6 include the data used to create the thickness and elevation surfaces. The correlation length of the thickness data was approximately 5,000 m, but the correlation among the data was not strong. This was especially the case at smaller distances. The weak

correlation and the large grid block size (several observations in one grid block) resulted in the interpolated surfaces departing from the observed data in some locations.

Table 3-1 HI interbed elevation and thickness data.

Well	Easting* (ft)	Northing* (ft)	Well Surface Elevation (m)	Depth to HI Interbed Top (m)	Hi Interbed Thickness (m)
cfa-1	295268	681593	1502.	190.	15.
cpp-3	296574	694817	1498.	158.	2.
cpp-4	297949	697486	1496.	159.	0.
lf2-09	294198	682901	1503.	190.	4.**
lf2-10	294274	682831	1503.	189.	15.
mtr-test	290310	701522	1499.	107.	0.
npr-test	312210	698222	1504.	169.	13.
ow-1	264794	665336	1537.	231.	2.
ow-2	264932	664910	1537.	238.	2.
rwmc-m04d	265512	667255	1531.	222.	1.
site-09	309853	677319	1502.	221.	26.
site-19	286464	701784	1502.	141.	2.
spert-IV	315027	685745	1501.	255.	27.
tra-06a	288954	698077	1501.	149.	2.
tra-07	288106	698380	1503.	151.	2.**
usgs-020	301200	686506	1499.	186.	20.**
usgs-034	292744	690801	1502.	181.	1.
usgs-038	293579	689569	1503.	182.	2.
usgs-039	292261	691692	1503.	173.	1.
usgs-040	295939	694541	1498.	161.	1.
usgs-041	295940	694140	1499.	162.	1.
usgs-042	295936	693637	1499.	167.	0.
usgs-043	295723	694859	1498.	157.	1.
usgs-044	295251	694237	1499.	159.	0.
usgs-045	295490	693598	1500.	165.	3.
usgs-046	295726	694027	1498.	165.	2.
usgs-047	296576	694114	1498.	162.	2.
usgs-048	296612	693414	1499.	167.	1.
usgs-049	297232	693640	1497.	165.	1.
usgs-051	296345	692344	1499.	171.	1.
usgs-052	297972	694833	1496.	160.	2.
usgs-057	294871	691753	1500.	173.	2.
usgs-058	290594	699503	1499.	104.	2.
usgs-059	297685	692760	1498.	169.	1.
usgs-065	288960	698169	1501.	149.	2.**
usgs-066	292672	697345	1500.	111.	2.
* Coordinates are: State Planar, Zone 3701, Datum NAD27					
** Well did not Fully Penetrate Interbed					

Table 3-1 continued HI interbed elevation and thickness data.

Well	Easting* (ft)	Northing* (ft)	Well Surface Elevation (m)	Depth to HI Interbed Top (m)	Hi Interbed Thickness (m)
usgs-067	298205	691728	1498.	174.	5.
usgs-076	290029	695977	1503.	161.	1.
usgs-079	286622	700079	1503.	148.	1.
usgs-082	300453	693410	1496.	170.	3.
usgs-083	295467	671394	1507.	218.	11.**
usgs-085	291436	685932	1505.	192.	2.**
usgs-104	295916	662585	1521.	210.	4.**
usgs-106	280997	669060	1529.	199.	0.
usgs-121	296600	698363	1496.	158.	2.
usgs-123	295776	692519	1500.	170.	1.
C-1A	269793	671707	1533.	213.	2.
EOCR	306147	677081	1507.	294.	10.
NPR_WO-2	312178	698359	1503.	174.	8.
S5G-Test	301655	722940	1478.	213.	8.
WS-INEL-1	294334	713220	1487.	204.	9.
* Coordinates are: State Planar, Zone 3701, Datum NAD27					
** Well did not Fully Penetrate Interbed					

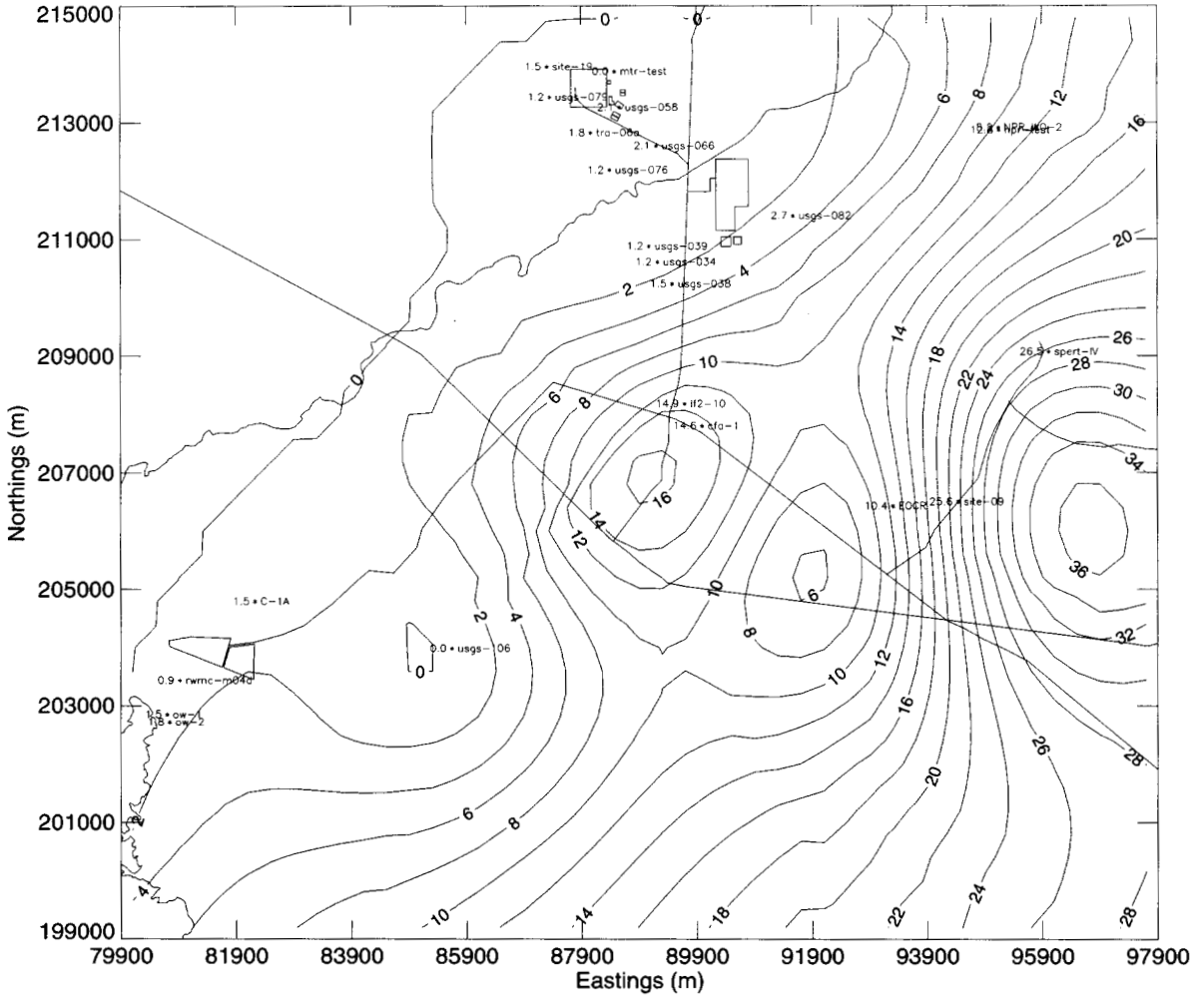

Figure 3-3 Simulated HI interbed thickness surface (m).

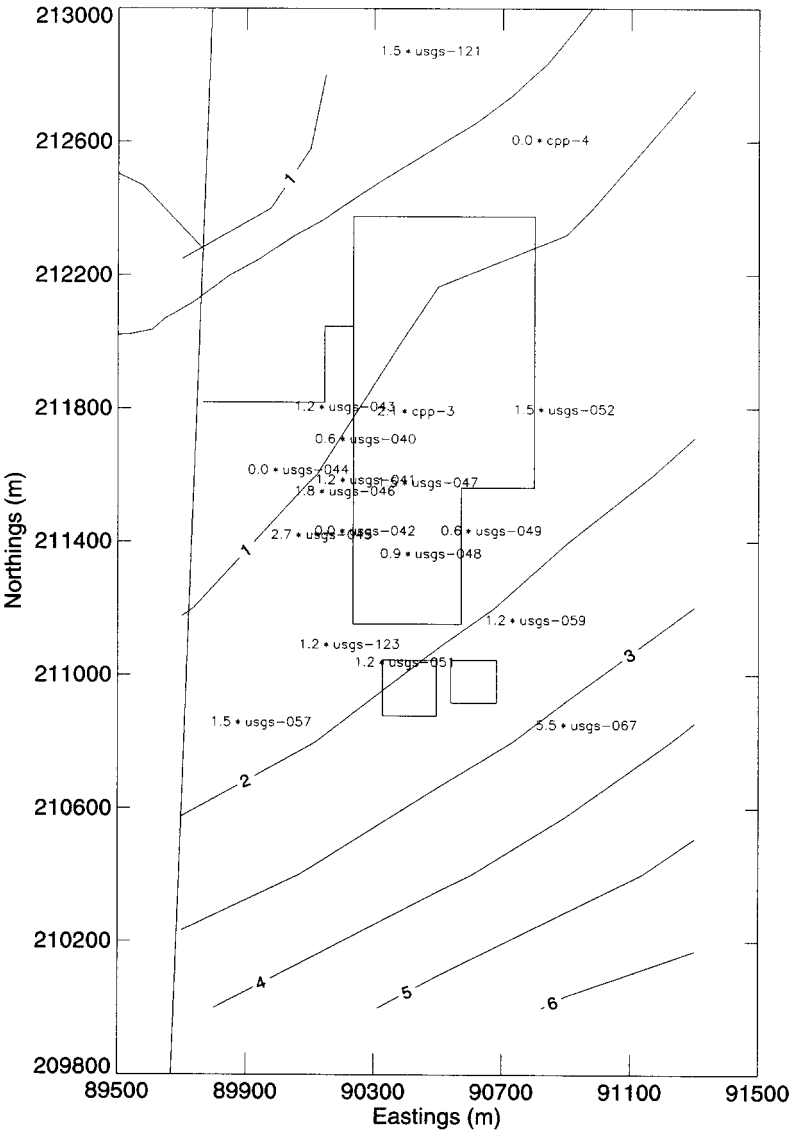

Figure 3-4 Simulated HI interbed thickness surface (m) in the INTEC vicinity.

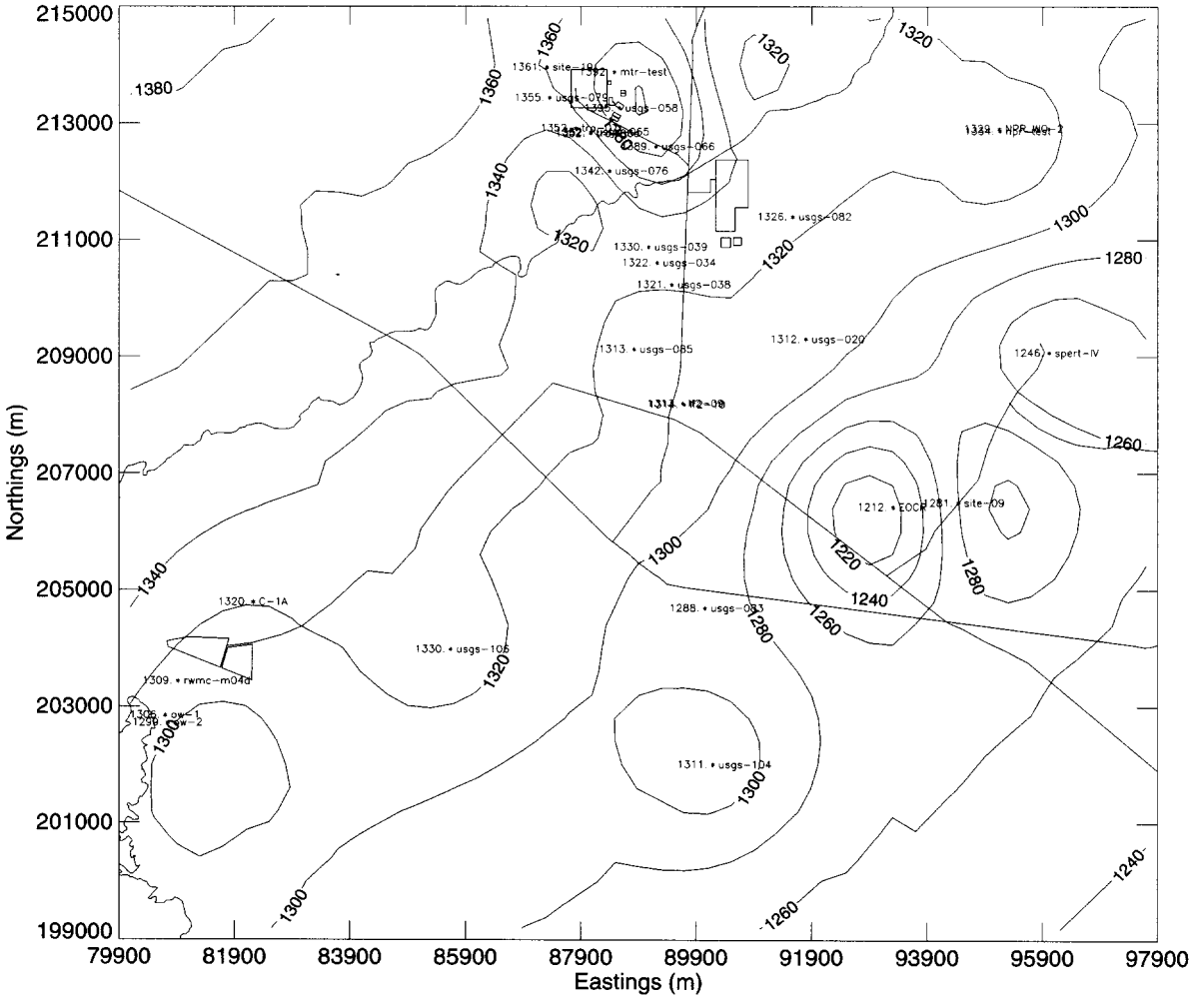

Figure 3-5 Simulated HI interbed surface elevation (m).

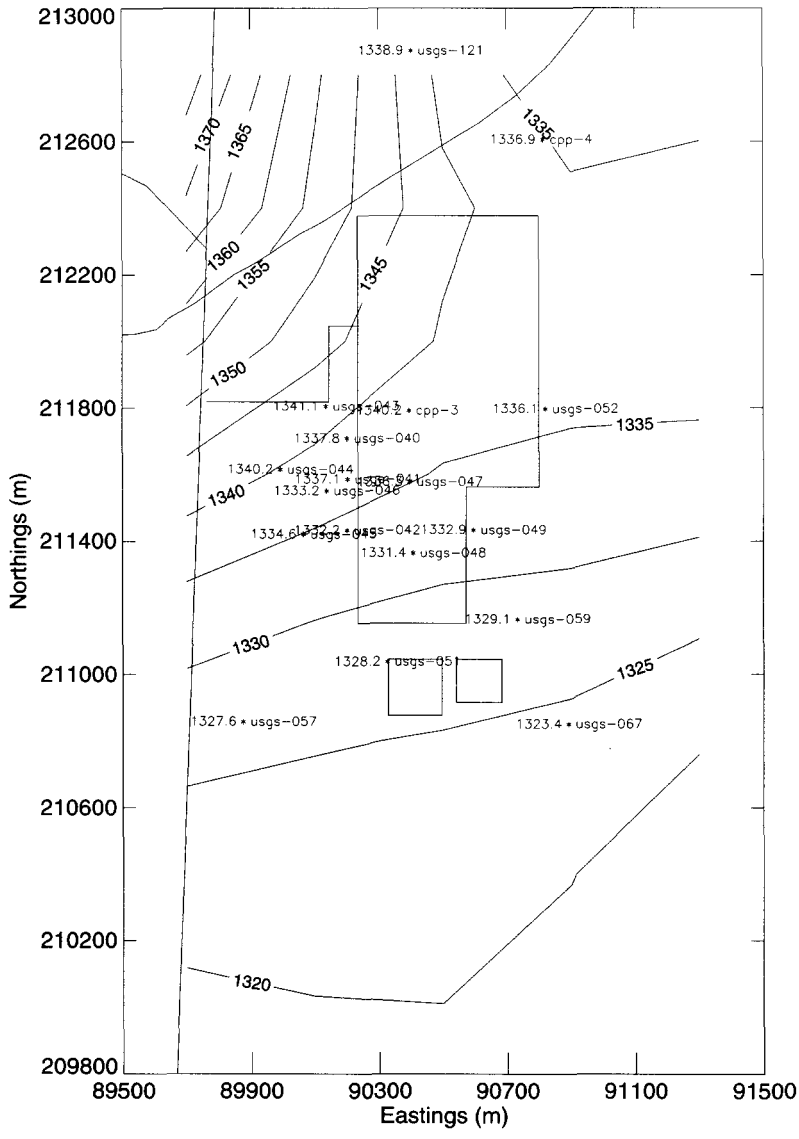

Figure 3-6 Simulated HI interbed surface elevation (m) in the INTEC vicinity.

3.1.2 HI Interbed Rediscretization

The updated model's vertical discretization follows the HI interbed to place more computational nodes in and around the HI interbed. Adapting the grid to follow the HI interbed also allows fewer computational nodes while adequately representing the complex lithology of the interbed. The interbed is represented by an average of four model layers, and the minimum thickness is 2 m. In some locations where the interbed is less than 6 m thick, fewer than 3 grid block are used to represent the interbed. This area is generally located northwest of a line between the SDA and INTEC percolation ponds. The need to maintain appropriate grid block aspect ratios (ratio of vertical to horizontal length) does not allow grid blocks less than 2 m thick. The grid block thickness increases with distance above and below the interbed and the updated model consisted of

18 layers. The vertical discretization is shown in Figure 3-7. The simulated HI interbed is illustrated by the red grid blocks.

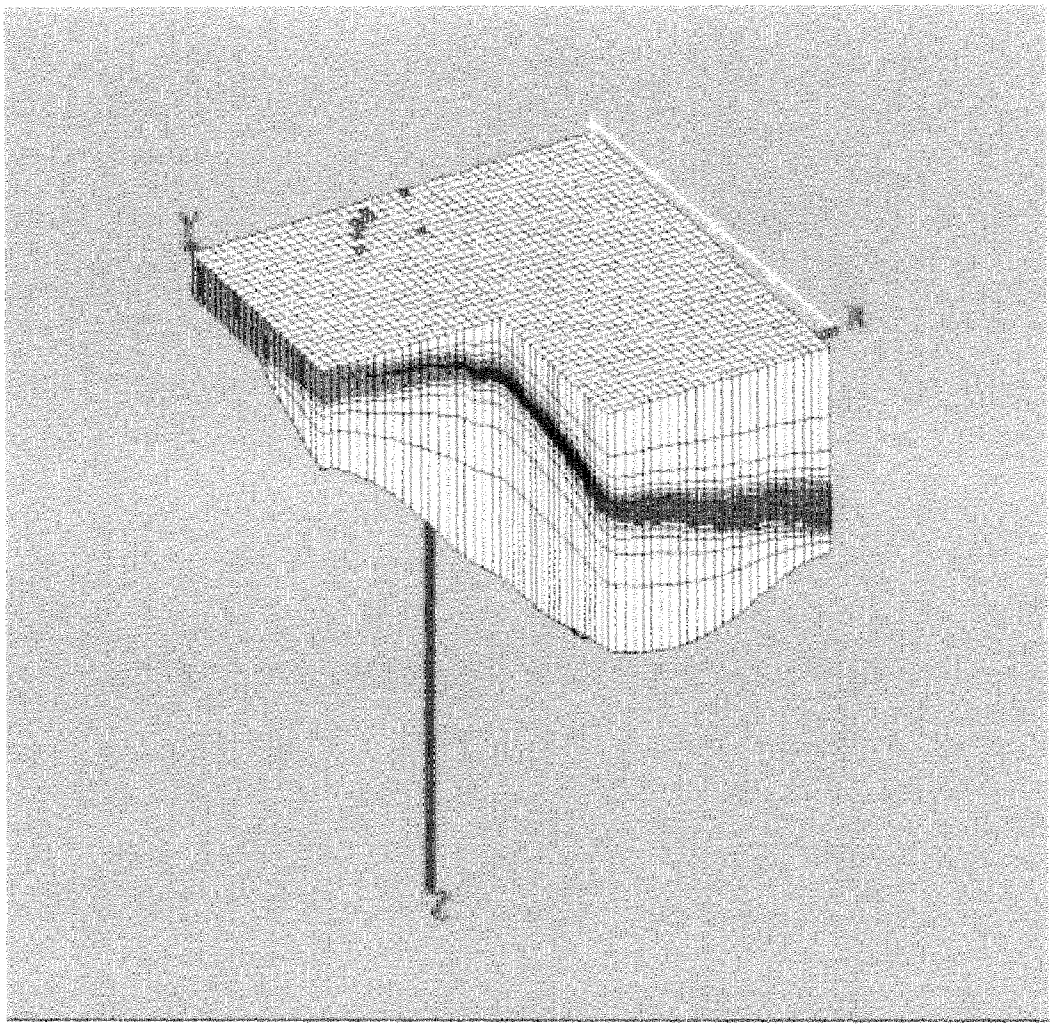

Figure 3-7 Updated aquifer model vertical discretization with vertical exaggeration.

3.1.3 Model Discretization Sensitivity Results

The discretization sensitivity simulations used the updated model's grid, but did not use the recalibrated model's hydrologic parameters. Parameterization of the rediscretized model, apart from the vertical discretization, was identical to the RI/BRA model. The rediscretized model predicts the peak aquifer I-129 concentration will be 0.26 pCi/L in the year 2095. This is in contrast to the OU 3-13 RI/BRA model, which predicted the peak concentration would be 3.0 pCi/L in the year 2095 and large area of the HI interbed south of the INTEC would remain above the 1 pCi/L beyond 2095. This is primarily due to the rediscretization of the HI interbed and placing the model bottom below the HI interbed. I-129 still persists in the rediscretized model's HI interbed, but to a lesser extent of that in the RI/BRA model. In both models, the I-129 takes a relatively long time to enter and exit the interbed compared to basalt. This is because of the low permeability (4 mD (0.01 ft/day) for the interbed vs. approximately 1.e+5 mD (243 ft/day) for the basalt) and high porosity (0.487 for the interbed vs. 0.0625 for the basalt). In the RI/BRA model, I-129 persists longer within and above the HI interbed because of low velocity areas created by the different HI interbed placement. It is important to note that the rediscretized model has not been calibrated to tritium disposal and breakthrough as the RI/BRA

model was. The I-129 plumes in both models are comparable. However, the axis of the rediscretized model's plume has shifted slightly westward.

Figure 3-8 illustrates the maximum vertical I-129 concentrations and the plume axis as predicted by the rediscretized model in year 2000 and 2095. Figures 3-9 and 3-10 illustrate vertical cross sections of the rediscretized model's plume axis for the years 1954, 1965, 1981, 2000, 2025, 2058, 2074 and 2095. The aquifer bottom is shown as a thick red line and the HI interbed is denoted by dashed lines. The 0.01, 0.1, and 1.0 pCi/L isopleths are illustrated by a thin dashed, thin, and thick black lines, respectively. The CPP-3 injection well was simulated as a fully screened well extending 40 m below the water table and is shown in Figures 3-9 and 3-10 as a vertical blue line in the upper left corner of each cross-section. The CPP-03 injection well is screened across the HI interbed, which is present approximately 25 m below the water table. Figures 3-9 and 3-10 use a 300 m vertical scale instead of the 100 m scale presented in the RI/BRA cross sections because of the increased rediscretized model's depth.

I-129 disposal begins in 1954 and by 1965, as with the RI/BRA model, the down gradient migration of I-129 in the HI interbed lags behind that in the surrounding basalt. However in the year 2058, clean water movement through the contamination area lags in the interbed and isolated high concentrations of I-129 persist in the interbed where aquifer velocity is low.

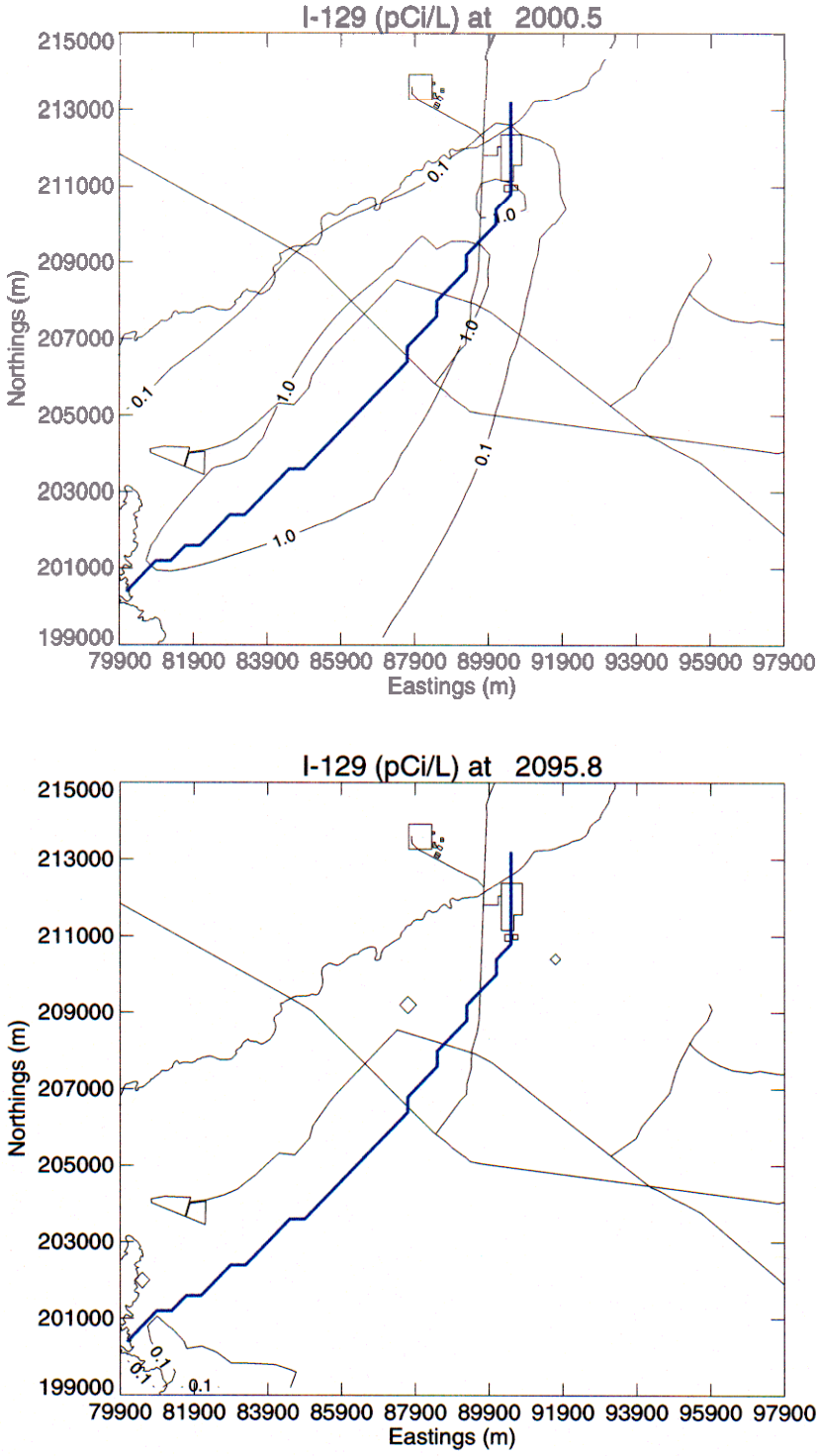

Figure 3-8 Rediscretized model maximum I-129 concentrations in 2000 and 2095 with plume axis (blue).

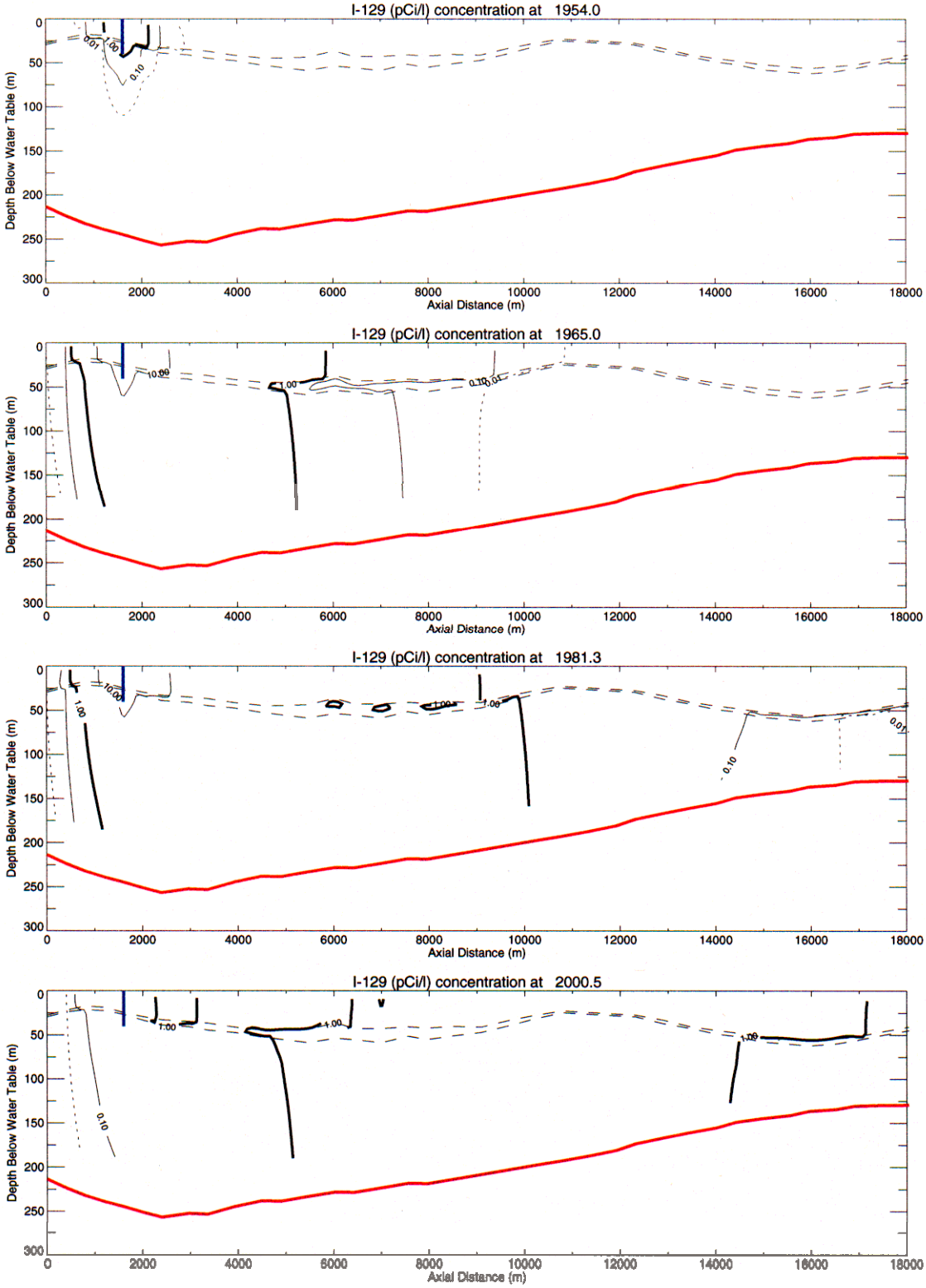

Figure 3-9 Rediscretized model plume axis vertical I-129 concentrations in 1954, 1965, 1981, and 2000 (the injection well is blue, the model bottom is red, and the long dashed black line represents the interbed).

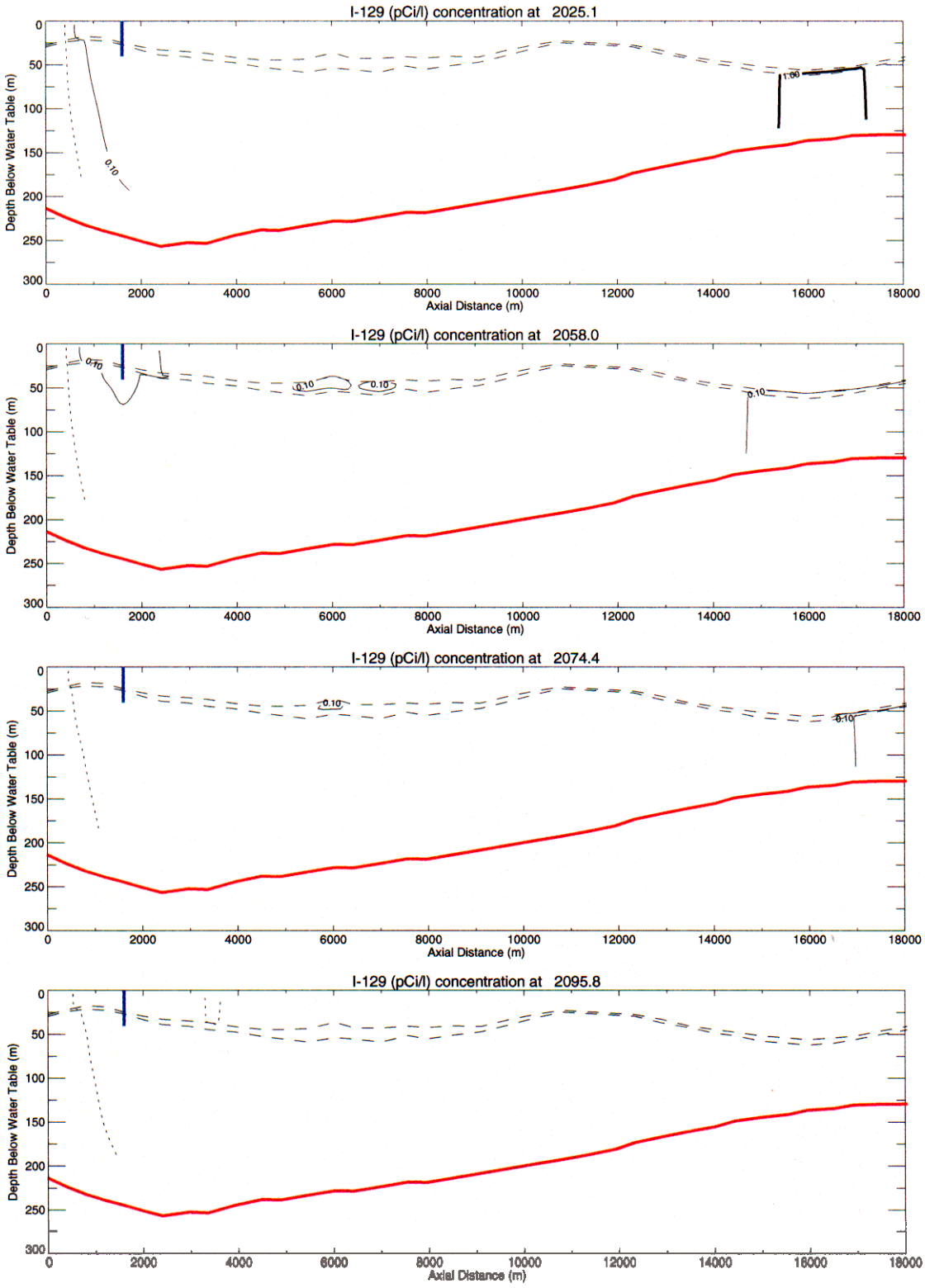

Figure 3-10 Rediscretized model plume axis vertical I-129 concentrations in 2025, 2058, 2074, and 2095 (the injection well is blue, the model bottom is red, and the long dashed black line represents the interbed).

3.2 Model Sensitivity to HI Interbed Permeability

The low permeability of the HI interbed is primarily responsible for maintaining elevated I-129 concentrations in the simulated Snake River Plain Aquifer. There is very little data available on the permeability of the HI interbed. The OU 3-13 RI/BRA aquifer modeling used a 4 mD (0.01 ft/d) interbed permeability from the RI/BRA vadose zone model calibration to perched water bodies beneath the INTEC. There is little confidence that vadose zone calibration adequately represents the HI interbed permeability within the aquifer. The existing permeability data for the HI interbed was reviewed and most representative permeability value along with reasonable bounds for the interbed permeability were estimated. The sensitivity of the RI/BRA and rediscretized model to HI interbed permeability using bounding values was evaluated to determine the value of gathering HI interbed permeability data.

3.2.1 Permeability Data Review

There is very little information available on the hydraulic conductivity of the HI interbed and the following tables include information available regarding other interbeds. WAG-3 OU 3-13 RI/BRA (DOE-ID, 1997) contained three tables with interbed hydraulic properties. The hydraulic conductivity information in those tables has been summarized, converted to permeability in millidarcies (mD) and presented in Table 3-2. In addition, in Table 3-3 is a summary of HI interbed hydraulic conductivities estimated by model calibration of pumping test results performed by the State of Idaho (Fredrick and Johnson, 1996). These pumping tests were done using packers to isolate the interbed from the surrounding basalt and are the only hydraulic conductivity information available specifically for the HI interbed.

Based on these interbed permeabilities, the 4 mD (0.01 ft/d) used for the WAG 3-13 modeling is relatively low. The HI interbed model calibration results shown in Table 3-2 (Frederick and Johnson, 1996) suggest the range is 37 mD (0.09 ft/d) to 100 mD (0.24 ft/d). Therefore, the 4 mD (0.01 ft/d) used for the WAG 3-13 modeling is at least an order of magnitude low. The other interbed permeability information ranges from 0.05 mD (0.0001 ft/d) to 3,500 mD (8.5 ft/d). An average permeability of 40 mD (0.10 ft/d) is on the low end of a the most appropriate permeability value. The 4 mD (0.01 ft/d) used in the RI/BRA modeling represents a low bounding value and 200 mD (0.49 ft/d) represents a high bounding value. A 200 mD (0.49 ft/d) permeability is approximately double the geometric mean all interbed permeability data provided in Table 3-2 and double the highest value in Table 3-3.

Table 3-2 Summary of interbed hydraulic conductivity data from the OU 3-13 RI report (DOE-ID,1997).

Well	Material	Average Permeability (mD)	Range of Permeability (mD)	(mD)	Reference
MW-2	Sandy clay interbed	1.86E+03	Single Value		OU 3-13 RI, Table 2-17
MW-4	Silty sand and gravel interbed	4.04E+01	Single Value		OU 3-13 RI, Table 2-17
MW-6	Silty sand, fine grained interbed	1.35E+03	Single Value		OU 3-13 RI, Table 2-17
MW-3	Silty clay	9.21E+01	Single Value		OU 3-13 RI, Table 2-18
MW-4	Silty sand and gravel	1.66E+01	Single Value		OU 3-13 RI, Table 2-18
MW-8	Clay with silt	1.14E+01	Single Value		OU 3-13 RI, Table 2-18
MW-10	Sandy silt	1.04E+01	Single Value		OU 3-13 RI, Table 2-18
MW-11	Silty sand	1.24E+01	Single Value		OU 3-13 RI, Table 2-18
MW-4	Silt	3.31E+01	Single Value		OU 3-13 RI, Table 2-18
MW-4	Silt	6.94E+01	Single Value		OU 3-13 RI, Table 2-18
Arithmetic mean		1.45E+03			
Geometric mean		8.86E+01			

Table 3-2 continued Summary of interbed hydraulic conductivity data from the OU 3-13 RI report (DOE-ID,1997).

Well	Material	Average Permeability (mD)	Range of Permeability (mD)	(mD)	Reference
MW-6	Clay	3.11E-01	Single Value		OU 3-13 RI, Table 2-18
MW-9	Clay with silt	2.17E+04	Single Value		OU 3-13 RI, Table 2-18
MW-11	Clay	5.38E-02	Single Value		OU 3-13 RI, Table 2-18
MW-3	silty clay	8.59E+02	Single Value		OU 3-13 RI, Table 2-18
MW-6	silty clay	2.28E+03	Single Value		OU 3-13 RI, Table 2-18
MW-9	silt with clay	3.52E+03	Single Value		OU 3-13 RI, Table 2-18
MW-1	sand with silt	3.42E+02	Single Value		OU 3-13 RI, Table 2-18
CD interbed		3.83E+01	3.11E-01	1.35E+03	OU 3-13 RI, Table 2-19
D interbed		1.35E+02	5.38E-02	3.52E+03	OU 3-13 RI, Table 2-19
deep interbed		3.42E+02	3.42E+02	3.42E+02	OU 3-13 RI, Table 2-19
TRA		1.45E+00	1.76E-02	1.45E+03	OU 3-13 RI, Table 2-19
RWMC		7.87E+01	7.87E+01	7.87E+01	OU 3-13 RI, Table 2-19
Arithmetic mean		1.45E+03			
Geometric mean		8.86E+01			

Table 3-3 Summary of calibrated HI interbed permeability values from Fredrick and Johnson, 1996.

Well	Permeability (mD)	Reference
USGS-44	9.99E+01	Fredrick and Johnson, 1996, Table 11
USGS-45	7.89E+01	Fredrick and Johnson, 1996, Table 11
USGS-46	7.89E+01	Fredrick and Johnson, 1996, Table 11
USGS-59	3.68E+01	Fredrick and Johnson, 1996, Table 11
arithmetic mean	73.62	
geometric mean	69.17	

3.2.2 Permeability Sensitivity Results

HI interbed permeability in the RI/BRA and rediscretized model was varied from 4 to 200 mD (0.01 to 0.5 ft/day) and peak concentrations and the size of the I-129 plume in 2095 were compared. The area of the remaining plume in 2095 is very sensitive to permeability and monotonically decreases in size with increasing permeability for both models. The RI/BRA model area of the 0.1pCi/L plume decreased from 70.6 to 45.4 Km^2 for the 4 and 200 mD (0.01 to 0.49 ft/day) interbed permeability, respectively. The rediscretized model 0.1 pCi/L area decreased from 4.32 to 0 Km^2 for the 4 and 200 mD (0.01 to 0.49 ft/day) simulations. The peak concentrations in the year 2095 did not monotonically decrease with increasing permeability. The RI/BRA model's peak values ranged from 2.1 pCi/L for the 8 mD (0.02 ft/day) permeability to 3.4 pCi/L for the 40 mD (0.1 ft/day) permeability simulation. The rediscretized model's peak values ranged from 0.09 pCi/L for the 200 mD (0.49 ft/day) simulation to 0.50 pCi/L for the 8 mD simulation. The varied peak concentrations in 2095 for the different interbed permeabilities indicate flow field substantially changes with different interbed permeabilities, which results in different areas retaining high I-129 concentrations. Only the RI/BRA 4 mD (0.01 ft/day) interbed permeability simulation was calibrated to tritium disposal in CPP-3 and breakthrough in down gradient wells. Table 3-4 provides maximum concentrations and the area of the I-129 plume with concentrations above 0.1 and 1.0 pCi/L.

Table 3-4 Permeability sensitivity year 2095 I-129 maximum concentrations and areal extent.

HI Interbed Permeability Sensitivity Simulation	RI/BRA Model			Rediscretized Model*		
	Maximum 2095 Concentration (pCi/L)	2095 Areal Extent of 0.1 pCi/L Plume (km^2)	2095 Areal Extent of 1 pCi/L Plume (km^2)	Maximum 2095 Concentration (pCi/L)	2095 Areal Extent of 0.1 pCi/L Plume (km^2)	2095 Areal Extent of 1 pCi/L Plume (km^2)
4mD	3.0	70.6	1.92	0.26	4.32	0.
8mD	2.1	64.8	0.80	0.50	2.08	0.
40mD	3.4	51.2	0.32	0.24	0.64	0.
200mD	3.1	45.4	0.96	0.09	0.	0.
*The rediscretized model used identical hydrologic properties as the RI/BRA. Only the model discretization was changed.						